FULL PAPER

Dalton
www.rsc.org/dalton

Equilibrium, kinetic and HPLC study of the reactions between platinum(II) complexes and DNA constituents in the presence and absence of glutathione

Živadin D. Bugarčić,*[a] Tanja Soldatović,[a] Ratomir Jelić,[a] Berta Algueró[b] and Anna Grandas*[b]

[a] *University of Kragujevac, Faculty of Science, Department of Chemistry, R. Domanovića 12, P. O. Box 60, Sr-34000 Kragujevac, Serbia. E-mail: bugi@kg.ac.yu*

[b] *Departament de Química Orgànica, Facultat de Química, Universitat de Barcelona, Martí i Franquès 1-11, 08028 Barcelona, Spain. E-mail: anna.grandas@ub.edu*

Received 21st July 2004, Accepted 7th October 2004
First published as an Advance Article on the web 22nd October 2004

The complex formation equilibria of $[Pt(SMC)(H_2O)_2]^+$ and $[Pt(terpy)H_2O]^{2+}$, where SMC = *S*-methyl-L-cysteine and terpy = 2,2′:6′,2″-terpyridine, with some biologically relevant ligands such as inosine (INO), inosine-5′-monophosphate (5′-IMP), guanosine-5′-monophosphate (5′-GMP) and glutathione (GSH) were studied. The stoichiometry and stability constants of the complexes formed are reported, and the concentration distribution of the various complex species have been evaluated as a function of pH. Also the kinetics and mechanism of the complex formation reactions were studied as a function of nucleophile concentration and temperature. For the complex $[Pt(SMC)(H_2O)_2]^+$, two consecutive reaction steps, which both depend on the nucleophile concentration, were observed under all conditions. The negative entropies of activation support an associative complex formation mechanism. Reaction of guanosine-5′-monophosphate (5′-GMP) with Pt(II) complexes was carried out in the presence and absence of glutathione (GSH) at neutral pH. The rate constants clearly showed a kinetic preference toward GSH at neutral pH. The reactions were also monitored by HPLC. However, only a small amount of coordinated 5′-GMP was detected in the HPLC trace. The products were isolated and characterized by MALDI-TOF mass spectrometry.

Introduction

The anticancer drugs, *cis*-diamminedichloroplatinum(II), *cis*-$[PtCl_2(NH_3)_2]$, cisplatin, or *cis*-diammine[1,1-cyclobutanedicarboxylato]-*O*,*O*′-platinum(II), carboplatin, are widely used for the treatment of testicular, ovarian, and other forms of cancer.[1,2] Although the anti-tumour activity of cisplatin or carboplatin, is ascribed to interactions between the complex and DNA,[2–4] a large amount of the platinum reacts with other biomolecules, such as proteins and enzymes. In fact, already in the blood, where the Pt drug is administered by injection or infusion, several molecules are available for kinetic and thermodynamic competition.[3,4] Sulfur containing molecules have a high affinity for platinum and could form very stable bonds. Moreover, the interaction of Pt complexes with sulfur containing biomolecules has been associated with negative phenomena and some drawbacks in the clinic still remain, such as nephrotoxicity, gastrointestinal toxicity, ototoxicity and neurotoxicity and drug resistance.[5–7] Reactions with thiol (SH) groups of protein side chains (*e.g.* in metallothionine and glutathione) are thought to trap and deactivate the drug before it reaches its cellular DNA target to form 1,2-intrastrand cross-links with guanine bases, the likely cytotoxic adduct.[8] Glutathione, a tripeptide with a sequence γ-glutamylcysteinylglycine (γ-Glu–CysH–Gly, GSH) is frequently the most prevalent intracellular thiol with concentrations up to 10 mM and it is the most abundant low molecular weight peptide. GSH has been adapted through evolution to perform many divers functions. For instance, GSH protects cells from the toxic effects of reactive oxygen compounds and is an important component of the system that uses reduced pyridine nucleotide to provide the cell with its reducing properties. GSH functions in catalysis, metabolism and transport. It participates in reactions involving the synthesis of proteins and nucleic acids and in those that detoxify free radicals and peroxides. The intracellular level of GSH is much greater than that of cysteine. Also, GSH serves as a storage and transport form of cysteine moieties. GSH is synthesized intracellularly and is exported from the cell.[9–11]

At present it is not clear how the platinum(II) species reaches DNA, because Pt(II) has a high affinity for sulfur donors as compared with nitrogen donor ligands such as those of the DNA nucleobases. The cysteine–platinum linkage is quite inert,[12] whereas methionine bonded to platinum can be replaced by thiols or nucleobases.[13–14] Studies on the interaction between the drug carboplatin and sulfur-containing biomolecules have shown that long-lived Pt–methionine adducts may be important metabolites *in vivo*.[15] It has been hypothesized that platinum might initially bind to sulfur-containing nucleophiles, and, in the case of the methionine adducts, migrate to DNA to form thermodynamically more stable products.[16–19] This assumption is supported by different experiments carried out with models of cisplatin,[3,20] but it is not confirmed by the results obtained in the experiments using cisplatin.[20] In these circumstances, more studies are required to understand the evolution of the reactions of platinum(II) complexes with naturally occurring compounds, and how platinum(II)-based anticancer drugs can reach their target.

The mono-functional $[PtCl(terpy)]^+$ and related complexes of the general type $[Pt(terpy)X]^{2+}$, terpy is 2,2′:6′,2″-terpyridine, are very useful models for studying the ligand substitution reactions of square-planar complexes. The kinetics of the substitution reactions involving several different X ligands have been investigated.[21–29] We have studied the kinetics of the complex-formation reactions between $[Pd(terpy)H_2O]^{2+}$ and $[Pt(terpy)H_2O]^{2+}$ with L-cysteine, DL-penicillamine, glutathione and thiourea.[28,29] Also, we recently published the results of the substitution reactions of the complexes $[Pt(terpy)H_2O]^{2+}$, $[Pt(terpy)(cyst\text{-}S)]^{2+}$ and $[Pt(terpy)(guo\text{-}N7)]^{2+}$, where cyst-S is L-cysteine and guo-N7 is guanosine, with some biologically relevant ligands such as inosine, inosine-5′-monophosphate, guanosine-5′-monophosphate, L-cysteine, glutathione, thiourea, thiosulfate and diethyldithiocarbamate in aqueous 0.10 M $NaClO_4$ at pH 2.5 and 6.0 using variable-temperature and -pressure stopped-flow spectrophotometry.[30] The complex, $[Pt(SMC)(H_2O)_2]^+$ has been chosen as a bi-functional complex. However, this complex has higher solubility and it is more reactive than cisplatin.

DOI: 10.1039/b411168k

With the aim of extending our earlier work, we have performed a detailed study of the complex-formation kinetics of $[Pt(SMC)(H_2O)_2]^+$ and $[Pt(terpy)H_2O]^{2+}$ where SMC is *S*-methyl-L-cysteine, with inosine, inosine-5′-monophosphate, guanosine-5′-monophosphate and glutathione in an aqueous solution. The evolution of the reaction of $[PtCl(terpy)]^+$ with 5′-GMP in the presence and absence of glutathione was monitored by reversed-phase HPLC and is also described here.

Experimental

Synthesis of complexes

The complexes $[PtCl(terpy)]Cl\cdot 2H_2O$ and $[PtCl_2(SMC)]$ were prepared according to a literature method.[31–33] Chemical analysis, UV-VIS and ^1H NMR spectral data were in good agreement with those obtained in previous preparations.

Chemicals and solutions

The chloro complex $[PtCl(terpy)]Cl\cdot 2H_2O$ or $[PtCl_2(SMC)]$, was converted into the aqua analogue in solution by addition of an equivalent of $AgClO_4$, heating to 40 °C for 1 h, and removing the AgCl precipitate by filtration through a 0.1 μm pore membrane filter. Great care was taken to ensure that the resulting solution was free of Ag^+ ions and that the chloro complex had been converted completely into the aqua species. Since it is known that perchlorate ions do not coordinate to Pt(II) and Pd(II) in aqueous solution,[34] the kinetics of the complex-formation reactions were studied in perchlorate medium. The ionic strength of the solutions was adjusted to 0.1 mol dm^{-3} with $NaClO_4$ (Merck, p.a.). The pH of the solutions was adjusted with $HClO_4$ and NaOH.

Ligand stock solutions were prepared shortly before use by dissolving the chemicals, glutathione (Fluka, assay > 99%), inosine, inosine-5′-monophosphate sodium salt hydrate, guanosine-5′-monophosphate sodium salt hydrate (Sigma). The other reagents were of AR quality. Highly purified, deionised water was used in the preparation of all solutions.

Instrumentation

Chemical analyses were performed on a Carlo Erba Elemental Analyzer 1106. UV-VIS spectra were recorded on Shimadzu UV 250 and Hewlett-Packard 8452A diode-array spectrophotometers with thermostatted 1.00 cm quartz Suprasil cells. Potentiometric measurements were performed using a Metrohm 686 titraprocessor equipped with a 665 dosimat. The electrode and titraprocessor were calibrated with standard buffer solutions prepared according to NBS specifications.[35] The pH meter readings were converted into hydrogen ion concentration by titrating a standard acid solution (0.01 mol dm^{-3}), the ionic strength of which was adjusted to 0.1 mol dm^{-3} with $NaClO_4$, with standard base (0.10 mol dm^{-3}) at 25 °C. The pH is plotted against p[H]. The relationship pH − p[H] = 0.05 was observed. The $[OH^-]$ value was calculated using a pK_w value of 13.997.[36] Kinetic measurements were carried out on a Hi-Tech stopped-flow spectrophotometer. Kinetic data were collected and analyzed using the OLIS KINFIT (Bogart, GA) set of programs.[37]

High pressure liquid chromatography (HPLC) was carried out using a Shimadzu system equipped with two LC-6A pumps, an SCL-6B controller, an SIL-6B autoinjector and a variable wavelength UV-Vis detector. Mass spectrometric characterization of the isolated compounds was accomplished by matrix-assisted laser desorption ionization time-of-flight (MALDI-TOF) analysis using an Applied Biosystems Voyager-DERP™ instrument (reflector, 337 nm laser, 3 ns pulses).

Potentiometric measurements

The acid-dissociation constants of the ligands were determined by titrating 2.5 × 10^{-3} mol dm^{-3} solution of each with standard NaOH solution. The hydrolysis constants of $[Pt(SMC)(H_2O)_2]^+$ complex was determined by titrating 2.5 × 10^{-3} mol dm^{-3} of the solution complex with NaOH. The formation constants of the complexes were determined by titrating solution mixtures of $[Pt(SMC)(H_2O)_2]^+$ (2.5 × 10^{-3} mol dm^{-3}) and the ligand in concentration ratios of 1:1 and 1:2 (complex:ligand). The titration solution mixtures had a volume of 40 ml. The titrations were carried out at 25 °C by circulating thermostatted water through the double-wall titration vessel and under a slow and constant stream of N_2 through the test solution. The ionic strength was adjusted to 0.10 mol dm^{-3} by $NaClO_4$. A 0.10 mol dm^{-3} NaOH solution was used as titrant. At the beginning of the titration the equilibrium was established in a few minutes (5–10), but when hydrolysis of the complexes has started the equilibrium required more time (1–2 h). The equilibrium constants for the species of the general formula $M_pL_qH_r$ (M = $[Pt(SMC)(H_2O)_2]^+$ or $[Pt(terpy)H_2O]^{2+}$ and L = glutathione, INO, 5′-IMP and 5′-GMP) were calculated using the program[36] MINIQUAD-75. The stoichiometry and stability constants of the complexes formed were determined by testing various possible composition models. The selected model gave the best statistical fit and was chemically consistent with the titration data without giving any systematic drifts in the magnitude of various residuals, as described elsewhere.[38] The results are summarized in Table 1. The species distribution diagrams were obtained using the program[39] SPECIES under the experimental conditions employed.

Table 1 Equilibrium constants for INO, 5′-IMP, 5′-GMP, and GSH complexes with $[Pt(SMC)(H_2O)_2]^+$ and $[Pt(terpy)(H_2O)]^{2+}$ at 25 °C; 0.1 mol dm^{-3} ionic strength

System	*p*	*q*	*r*[a]	log *β*[b]
$[Pt(SMC)(H_2O)_2]^+$	1	0	−1	−3.49(0.02)
	1	0	−2	−12.29(0.03)
	2	0	−1	−0.06(0.06)
INO	0	1	1	8.68(0.06)
	1	1	0	8.23(0.02)
	1	2	0	12.20(0.03)
5′-IMP	0	1	1	9.14(0.05)
	0	1	2	15.25(0.03)
	0	1	3	16.33(0.08)
	1	1	0	9.61(0.05)
	1	1	1	15.87(0.06)
5′-GMP	0	1	1	9.59(0.07)
	0	1	2	15.73(0.05)
	0	1	3	18.06(0.06)
	1	1	0	12.38(0.04)
	1	1	1	18.80(0.05)
	1	1	2	22.27(0.05)
GSH	0	1	1	9.73(0.05)
	0	1	2	18.06(0.07)
	0	1	3	21.58(0.09)
	0	1	4	23.68(0.10)
	1	1	1	20.48(0.08)
	1	1	2	22.33(0.07)
	1	1	0	16.63(0.09)
$[Pt(terpy)(H_2O)]^{2+}$	1	0	−1	−4.42 (Ref. 21)
5′-GMP	0	1	1	9.59(0.07)
	0	1	2	15.73(0.05)
	0	1	3	18.06(0.06)
	1	1	1	15.85(0.03)
	1	1	2	21.25(0.05)
GSH	0	1	1	9.73(0.05)
	0	1	2	18.06(0.07)
	0	1	3	21.58(0.09)
	0	1	4	23.68(0.10)
	1	1	3	28.43(0.09)
	1	1	2	24.90(0.06)

[a] *p*, *q* and *r* are the stoichiometric coefficients corresponding to $[Pt(SMC)(H_2O)_2]^+$ or $[Pt(terpy)H_2O]^{2+}$, ligand and H^+, respectively. [b] Standard deviations are given in parentheses.

Kinetics

Spectral changes resulting from mixing platinum(II) complex and ligand solutions were recorded over the wavelength range

220 to 450 nm to establish a suitable wavelength at which kinetic measurements could be performed. Reactions were initiated by mixing equal volumes of the complex and ligand solutions directly in the stopped-flow instruments and were followed for at least 8 half-lives. Complex formation was monitored as an increase in absorbance at 340 nm, under pseudo-first order conditions with ligand in at least a 10-fold excess, and at pH 2.5 where the complex $[Pt(SMC)(H_2O)_2]^+$ exists in the aqua form. Complex formation of the $[PtCl(terpy)]^+$ was studied at pH *ca.* 6. The ionic strength of the reaction mixtures was kept constant at 0.1 mol dm^{-3} with $NaClO_4$. The temperature was controlled throughout all kinetic experiments to ± 0.1 °C. The observed pseudo-first-order rate constants, k_{obsd}, were calculated as the average of three to seven independent kinetic runs.

HPLC Studies

$[PtCl(terpy)]^+$ was first reacted with GSH or 5′-GMP, either in equimolar amounts or in a 1:2 ratio to ensure complete reaction. The adducts formed were isolated by HPLC using the same conditions described to monitor the reaction progress (see below). Reaction with a mixture of the three compounds in a relative proportion of Pt(II)/GSH/5′-GMP 1:1:12 was also carried out. In all cases the mixture of products was incubated in water at 37 °C for up to seven days, and the platinum(II) complex concentration was 1 or 2 mmol dm^{-3}.

The evolution of the reaction mixtures was monitored by reversed-phase HPLC, using a Kromasil C18 column (5 μm, 0.4 × 10 cm) and a linear gradient from 0 to 100% of *B* in 10 min (solvent *A*: 0.045% trifluoroacetic acid in H_2O, solvent *B*: 0.036% trifluoroacetic acid in acetonitrile, flow: 1 ml min^{-1}, detection wavelength: 244 nm). Retention times: Pt–N7 adduct: 5.4 min, $[PtCl(terpy)]^+$: 5.9 min, Pt–S adduct: 6.1 min.

The aliquots separated from the reaction mixture at different incubation times were kept frozen prior to analysis under the described conditions. Peaks with the same retention time between different runs were collected and lyophilized. All the isolated products were characterized by MALDI-TOF mass spectrometric analysis, where M is the mass of the adduct formed by $[Pt(terpy)]^{2+}$ and a negatively charged ligand.

MALDI-TOF mass spectrometric analysis

Ionization of platinum adducts was carried out in the positive mode using 2,5-dihydroxybenzoic acid as the matrix. In general, 0.02–0.1 OD units of the platinum adduct were solubilized in 20 μL H_2O for characterization assays. 1 μL of the matrix solution (10 mg in 1 mL of acetonitrile) was added to 1 μL of the sample solution, and after mixing by withdrawing and expelling the solution with a pipette several times, 1 μL of the resulting solution was spotted on the sample plate and dried. Typical isotopic distribution was observed, and the highest isotopic peak was taken as $[M]^+$, where M is the mass of the adduct [Pt(terpy)(L)].

Results and discussion

Equilibrium studies

The acid–base equilibrium of $[Pt(terpy)H_2O]^{2+}$ and $[Pt(SMC)(H_2O)_2]^+$ were characterized by fitting the potentiometric titration data to various acid–base models. The best model, selected according to the above mentioned method of calculation, was consistent with the deprotonation of one or two coordinated water molecules and formation of hydroxo and μ-hydroxo species, as given by eqn. (3).

$$\underset{100}{[Pt(terpy)H_2O]^{2+}} \rightleftharpoons \underset{10-1}{[Pt(terpy)(OH)]^{+}} + H \quad (3a)$$

$$\underset{100}{[Pt(SMC)(H_2O)_2]^{+}} \rightleftharpoons \underset{10-1}{[Pt(SMC)(H_2O)(OH)]} + H^+ \quad (3b)$$

$$\underset{10-1}{[Pt(SMC)(H_2O)(OH)]} \rightleftharpoons \underset{10-2}{[Pt(SMC)(OH)_2]^-} + H^+ \quad (3c)$$

$$2\underset{100}{[Pt(SMC)(H_2O)_2]^{+}} \rightleftharpoons \underset{20-1}{[Pt_2(SMC)_2(H_2O)_2(OH)]^{+}} + H^+ \quad (3d)$$

The pK_a value of the carboxylic acid group of coordinated *S*-methyl-L-cysteine was too low to be determined potentiometrically. The pK_a of coordinated water in $[Pt(terpy)H_2O]^{2+}$ is −4.42[21] and pK_{a1} and pK_{a2} of $[Pt(SMC)(H_2O)_2]^+$ are −3.49 and −8.80. pK_{a1} corresponds to deprotonation of the coordinated water molecule *trans* to the coordinated amino group, Table 1. pK_{a2} has a significantly higher value than the corresponding Pt–diamine complexes. This is due to the strong *trans* labilization effect of sulfur on the coordinated water molecule. The μ-hydroxo species (20−1) is assumed to form through dimerization of the Pt(II) complex *via* a hydroxo group bound in the positions *trans* to the coordinated amino group. A dimer with a single hydroxo bridge is formed with $[Pt(SMC)(H_2O)_2]^+$. The dimerization reaction can be reformulated as:

$$\underset{100}{[Pt(SMC)(H_2O)_2]^{+}} + \underset{10-1}{[Pt(SMC)(H_2O)(OH)]} \rightleftharpoons \underset{20-1}{[(SMC)(H_2O)Pt-OH-Pt(H_2O)(SMC)]^{+}} \quad (3e)$$

The equilibrium constant (*K*) for the dimerization reaction was determined to be log K = 3.43 (= log β_{20-1} − log β_{10-1}). The equilibrium constant for the corresponding dimerization of $[Pd(SMC)(H_2O)_2]^+$ was previously found to be log K = 4.12.[33] The difference may be explained in terms of the difference in Lewis acidity of Pd(II) and Pt(II).

The species distribution diagram for the hydrolyzed species of $[Pt(SMC)(H_2O)_2]^+$ is shown in Fig. 1.

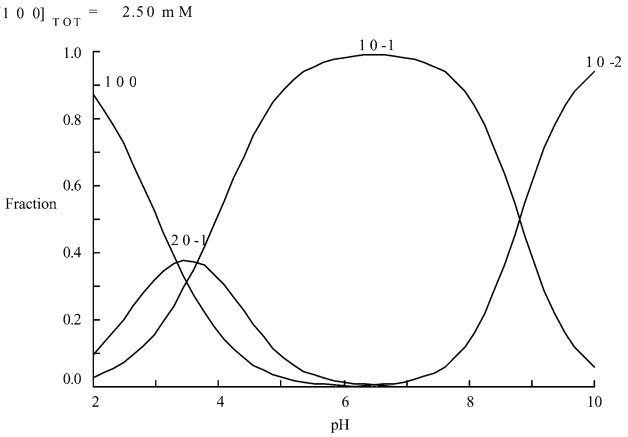

Fig. 1 Distribution of various species as a function of pH in the $[Pt(SMC)(H_2O)_2]^+$ system.

The concentration of the μ-hydroxo (20−1) and monoxydroxo (10−1) species increases with increasing pH. However, the dihydroxo (10−2) species starts to form at pH 6.2. The main species present under physiological conditions is the monohydroxo, which can interact with DNA constituents.

Complex-formation equilibria of $[Pt(SMC)(H_2O)_2]^+$ with DNA constituents

The purines, inosine, inosine-5′-monophosphate and guanosine-5′-monophosphate have two metal ion binding sites, *vs.* N_1 and N_7. The pH-dependent binding of these N-donors has been reported before.[40] The results show that inosine forms 110 and 120 complexes, Table 1. The 110 species is formed in the acidic pH range and corresponds to the N_7 coordinated complex, whereas the N_1 nitrogen is in the protonated form. The stability constants of the species 110 is, log β_{110} = 8.23, and for the 120 species is, log β_{120} = 12.20.

The distribution diagram for the inosine complex is given in Fig. 2. From Fig. 2 it can be seen that INO cannot suppress the hydrolysis, and the hydroxo species are present in solution. The complex 10−1 is present in the solution in the pH range between 2 and 10, and the maximum of the concentration is

about 5.5 with the concentration a little higher than 20%. The complex with INO 110 starts to form at pH 1 and reaches its maximum concentration at pH 5, where the formation of the complex 120 starts. The highest concentration of this complex is at about pH 8.5.

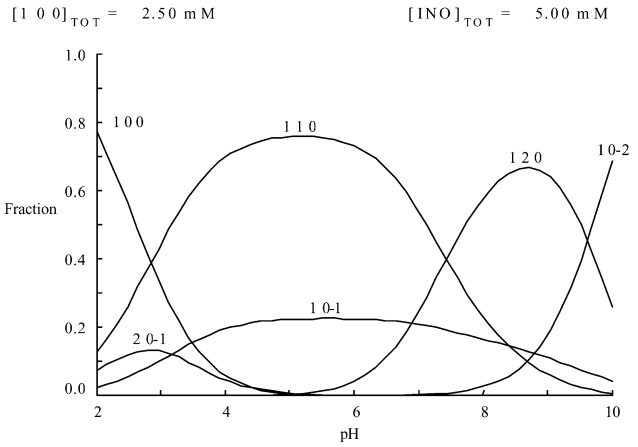

Fig. 2 Distribution of various species as a function of pH in the Pt(SMC)–INO system.

5′-IMP forms 111 and 110 complexes with log $\beta_{111} = 15.87$ and log $\beta_{110} = 9.61$, respectively. By comparison of the stability constants of the complex 110, of INO and 5′-IMP, it can be seen that the complex with 5′-IMP is more stable. There is no 120 complex and this could be explained by the steric effect of the phosphate groups.

From Fig. 3, it can be seen that the complex formation starts by formation of 111 complex, at pH 1, and the maximum of the concentration is at about 5. The complex 110 started at pH 4, and the maximum of the concentration reached at pH 8. Similarly, as in the case of INO, 5′-IMP cannot suppress the hydrolysis of $[Pt(SMC)(H_2O)_2]^+$. The hydroxo species, 10−1, is present in the pH range from 2 to 10, and the maximum of the concentration (about 20%) is at pH 7. At the physiological pH, the complex 110 is present in the highest concentration.

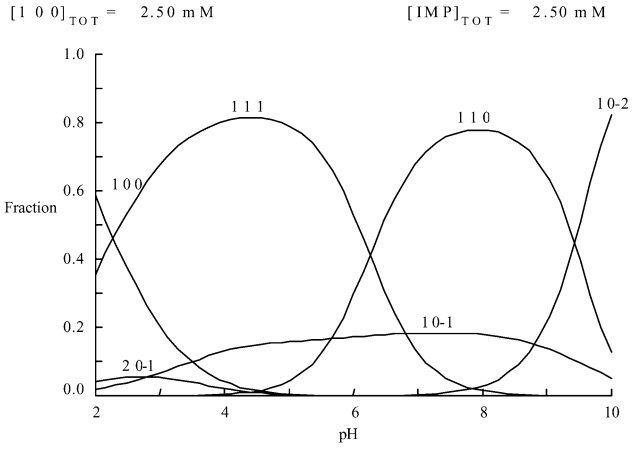

Fig. 3 Distribution of various species as a function of pH in the Pt(SMC)–IMP system.

5′-GMP forms complexes with stoichiometric coefficients of 110, 111 and 112, whereas hydroxo species are not formed at all. In the complex 112, 5′-GMP is protonated with two protons at the phosphate group, while in the case of the complex 110, 5′-GMP is deprotonated, see Fig. 4. However, in this case the hydrolysis of the aqua complex, $[Pt(SMC)(H_2O)_2]^+$, is suppressed.

The stability constants of the complexes, 110, 111 and 112, are: log $\beta_{110} = 12.38$, log $\beta_{111} = 18.80$ and log $\beta_{112} = 22.27$. From the distribution diagram, Fig. 4, it can be seen that the formation of the complex 112 started at acidic medium and at pH 6 it disappeared. The complex 111 forms at pH between 2 and 8,

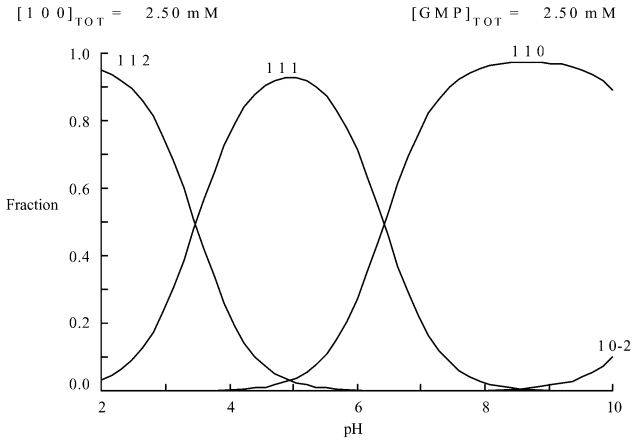

Fig. 4 Distribution of various species as a function of pH in the Pt(SMC)–GMP system.

with maximum of the concentration at pH 5. The complex 110, started at pH 5 and the maximum of the concentration is at pH 9. At physiological pH there are two complexes, 111 and 110, with a little higher concentration of 110.

The pK_a values of the protonated 5′-GMP complex are 6.42 (log β_{111} − log β_{110}) and 3.47 (log β_{112} − log β_{111}). These values correspond to the PO_2-OH and N_1H groups, respectively. The latter assignment is based on the fact that N_7 is coordinated to Pt(II), and as a result N_1H is acidified and its pK_a value is lowered significantly. The pK_a of protonated 5′-IMP complex is 6.26. This value may correspond to an average of the pK_a values for PO_2-OH and N_1H groups. It should be noted that the 5′-GMP complex (110) is significantly more stable than the inosine and 5′-IMP complexes, Table 1. This may be plausible due to hydrogen bonding between the exocyclic amino group of 5′-GMP and the carboxylic group of coordinated *S*-methyl-L-cysteine. This interaction will contribute to the stability of the formed complex.

It could be conclude that 5′-GMP forms highly stable complexes in comparison with INO and 5′-IMP, Table 1. The stability order is: INO < 5′-IMP < 5′-GMP.

Finally, a comparison of the stability constant values obtained from potentiometric and kinetic data are made for 5′-GMP. The stability constant of the 1:1 complex formed in the acidic pH range (where N7 is coordinated) obtained from potentiometric measurements log $K_1 = 3.47$ (log β_{112} − log β_{111}) is in good agreement with the values obtained from kinetic investigations, *viz.* log $K_1 = 3.02$ ($= k_1/k_{-1}$). In the case of INO and 5′-IMP this comparison could not be done because the complexes 111 and 112, respectively, have not been found.

Complex-formation equilibria of $[Pt(SMC)(H_2O)_2]^+$ with glutathione

In the reaction of $[Pt(SMC)(H_2O)_2]^+$ with glutathione (GSH) complexes with stoichiometry coefficients of 112, 111 and 110 have been found. The stability constants are: log $\beta_{112} = 22.33$, log $\beta_{111} = 20.48$ and log $\beta_{110} = 16.63$. (Table 1). From Fig. 5, the distribution diagram for this equilibrium can be seen. At acidic medium the predominant species is 112, fully protonated GSH, with a maximum of concentration at pH 3. The complex 111 is also present in acidic medium, but with a concentration of about 20%, with a maximum of concentration at pH 2. However, in acidic medium the dinuclear μ-hydroxo complex has been detected, 20−1, with a very small concentration. The formation of the complex 110, started at pH 2, and with increasing the pH, the concentration of this complex increased. The highest concentration of this complex is at physiological pH.

Complex-formation equilibria of $[Pt(terpy)H_2O]^{2+}$ with DNA constituents

The complex formation of the monofunctional complex, $[Pt(terpy)H_2O]^{2+}$ with 5′-GMP has been studied as a model for

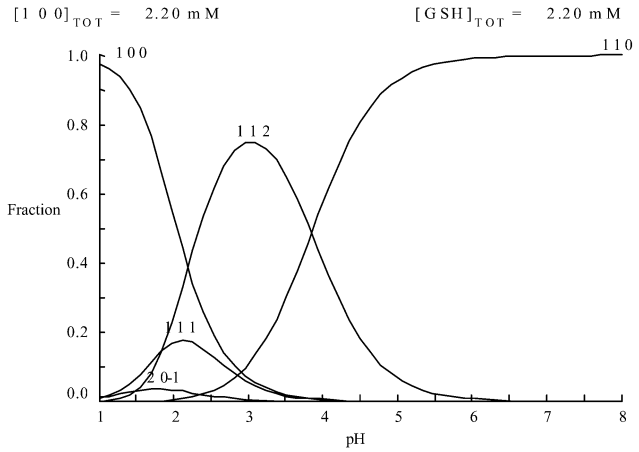

Fig. 5 Distribution of various species as a function of pH in the Pt(SMC)–GSH system.

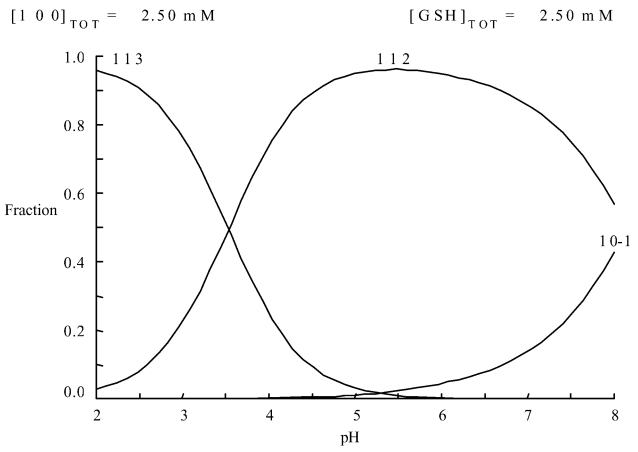

Fig. 7 Distribution of various species as a function of pH in the Pt(terpy)–GSH system.

the bifunctional $[Pt(SMC)(H_2O)_2]^+$. In this case, the complexes $[Pt(terpy)(5'\text{-GMP})]^{z+}$, with stoichiometry 111 and 112 where 5′-GMP is protonated with one (111) and two protons (112) have been found. The stability constants for these complexes are: $\log \beta_{111} = 15.85$ and $\log \beta_{112} = 21.25$. From the distribution diagram, Fig. 6, it can be seen that complex 112 forms at acidic medium with a maximum concentration at pH 3, while the complex 111 started at pH 3, and the maximum of the concentration is at pH 6.5. Also, it can be seen that at the same time as the formation of the 111 complex, the formation of the hydroxo complex 10−1, $[Pt(terpy)OH]^+$started. With increasing pH the concentration of this complex increases as well.

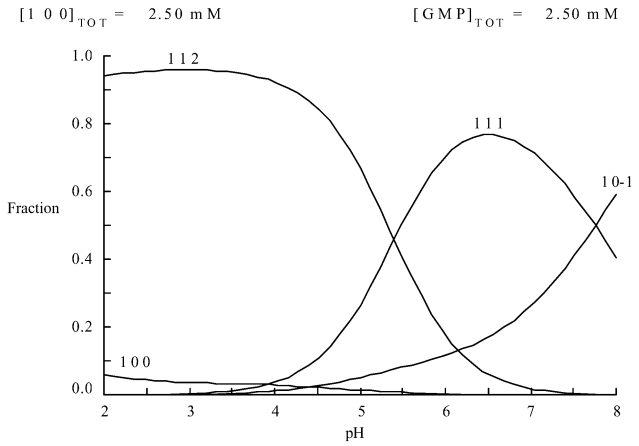

Fig. 6 Distribution of various species as a function of pH in the Pt(terpy)–GMP system.

Complex-formation equilibria of $[Pt(terpy)H_2O]^{2+}$ with glutathione

It is known that the complex $[Pt(terpy)H_2O]^{2+}$ does not react with thioethers,[23,24,41] so we studied the complex formation with thiols, GSH. In the present system the protonated complexes 113 and 112 have been found, with stability constants: $\log \beta_{113} = 28.43$ and $\log \beta_{112} = 24.90$. From the distribution diagram, Fig. 7, it can be seen that the complex 113 (with fully protonated GSH) is present in acidic medium, up to pH 5.5. The formation of the complex started at pH <2, while the maximum of the concentration is at pH 5.5. However, the hydroxo complex $[Pt(terpy)OH]^+$, 10−1, is present at pH >4. The concentration of this complex increases with increasing pH.

Kinetic studies for the complex formation of $[Pt(SMC)(H_2O)_2]^+$ with DNA constituents

The kinetics of the substitution of coordinated water was followed spectrophotometrically by following the change in absorbance at suitable wavelengths as a function of time. The reaction of $[Pt(SMC)(H_2O)_2]^+$ with the selected nucleophiles occurs in two subsequent steps. Both reaction steps exhibit linear dependence of k_{obsd} on the nucleophile concentration (see Fig. 8). This suggests that both substitution processes are reversible and proceed according to the reactions given in eqns. (5) and (6). The observed rate constants for the two reactions can be expressed as given in eqn. (7).

$$[Pt(SMC)(H_2O)_2]^+ + Nu \rightleftharpoons [Pt(SMC)(Nu)(H_2O)]^+ \quad (5)$$

$$[Pt(SMC)(Nu)(H_2O)]^+ + Nu \rightleftharpoons [Pt(SMC)(Nu)_2]^+ + H_2O \quad (6)$$

$$k_{obsd1} = k_{-1} + k_1[Nu] \text{ and } \quad k_{obsd2} = k_{-2} + k_2[Nu] \quad (7)$$

Values for the rate constants and thermal activation parameters estimated from the data in Fig. 8 are summarized in Table 2.

The activation parameters $\Delta H^{\ddagger}$ and $\Delta S^{\ddagger}$ were calculated using the Eyring equation. The reaction for the second step is significantly slower than for the first one. The faster reaction step with the larger absorption change was attributed to the substitution of the first coordinated H_2O in the *trans* position to the S donor atom of *S*-methyl-L-cysteine, whereas the slower reaction was assigned to the displacement of the other H_2O molecule. This is due to the strong *trans* labilization effect of coordinated sulfur. Inosine (INO), inosine-5′-monophosphate (5′-IMP) and guanosine-5′-monophosphate (5′-GMP) can coordinate to metal ions *via* N_1 and N_7. Under our experimental conditions (pH = 2.5) only the N_7 position of INO, 5′-IMP and 5′-GMP will bind to the central metal atom, since at this pH the N_1 position is protonated.[42,43] Binding through the N_7 position in a neutral or weakly acidic medium has been verified.[44] On average, k_1 is *ca.* 10^2 times faster than k_2, whereas k_{-1} is on average *ca.* 10 times faster than k_{-2} with the result that K_1 ($= k_1/k_{-1}$) is *ca.* 10 times larger than K_2 ($= k_2/k_{-2}$).

The introduction of an *S*-amino acid ligand into the Pt(II) or Pd(II) coordination sphere results in an increase in substitution reactivity. Such a labilization has clearly been illustrated by an earlier study.[33] The kinetic data clearly show that 5′-GMP is more reactive toward $[Pt(SMC)(H_2O)_2]^+$ than either INO and 5′-IMP. The forward and reverse reactions for both reaction steps (5) and (6) are characterized by significantly negative activation entropies, which is in line with an associative substitution mechanism.

The substitution behavior of the $[Pt(SMC)(H_2O)_2]^+$ complex is very similar to that reported for the related Pd(II) complex,[33] only Pd(II) analogs are *ca.* 10^3 times faster.

Kinetic studies for the complex formation of $[PtCl(terpy)]^+$ with DNA constituents and glutathione

The results of the substitution reactions of the $[Pt(terpy)H_2O]^{2+}$ complex with INO, 5′-IMP and 5′-GMP have been very recently

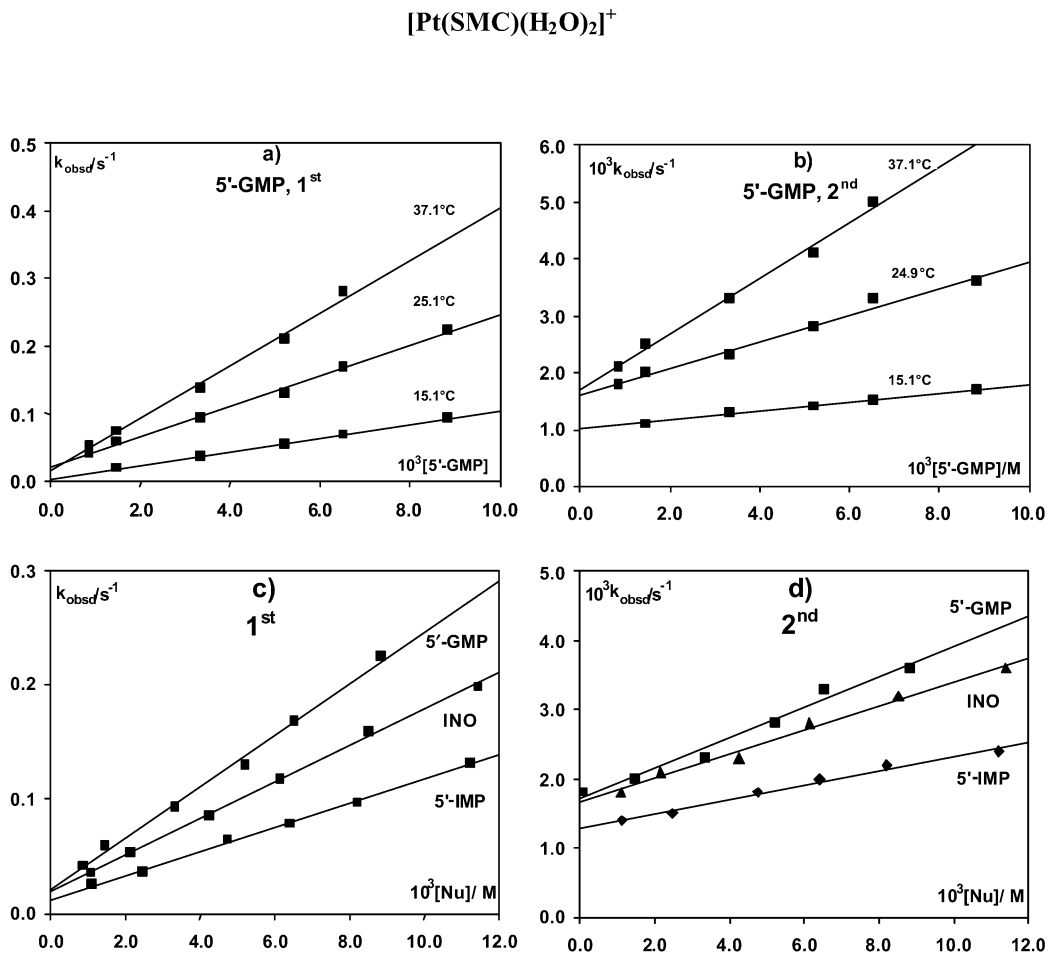

Fig. 8 Observed pseudo-first order rate constants, k_{obsd}, for the first and second reactions, as a function of nucleophile concentration and temperature (a and b); k_{obsd}, as a function of nucleophile concentration at 25 °C (c and d).

published.[30] The kinetic data clearly show that these ligands are very good nucleophiles for the $[Pt(terpy)H_2O]^{2+}$ complex, and that 5′-GMP is more reactive.[30] Also, the kinetics have been studied for the complex formation of the $[Pt(terpy)H_2O]^{2+}$ with thiols in aqueous 0.10 M perchloric acid.[28] GSH is the strongest nucleophile. Moreover, GSH is considerably more reactive than expected. From a comparison of the reactivity of thiols (L-cysteine, DL-penicillamine and glutathione)[28] with INO, 5′-IMP and 5′-GMP in reaction with $[Pt(terpy)H_2O]^{2+}$, it can be concluded that these N-bonding ligands are even better nucleophiles than the thiols mentioned.[30] The preference of these N-bonding nucleophiles over thiols in acidic solutions needs to be addressed. It must be borne in mind that the reactions with thiols have been investigated at pH 1, where all thiols were protonated. On the other hand, at pH 2.5 the N7 sites of INO, 5′-IMP and 5′-GMP are not protonated.

In this work, we have studied kinetics for the complex formation of the $[PtCl(terpy)]^+$ with 5′-GMP in the presence and absence of GSH at pH *ca.* 6, with a concentration ratio $[PtCl(terpy)]^+$:GSH:5′-GMP of 1:2:10. The observed pseudo-first-order rate constants, k_{obsd}, as a function of the total concentration of nucleophile are described by eqn. (8).

$$k_{obsd} = k_1 + k_2[\text{nucleophile}] \quad (8)$$

A least-squares fit of the data according to eqn. (8), resulted in values for the forward anation rate constants, k_2, and the reverse aquation rate constant, k_1.[45] The substitution reactions are characterized by almost zero values for k_1 (see Fig. 9). Thus, the complex-formation reaction for the GSH goes almost to completion. Linear plots of the observed pseudo-first-order rate constants k_{obsd} *versus* the total concentration of the GSH pass almost through the origin. The intercept is very small within the experimental error limits (Fig. 9a, c), illustrating that the solvent cannot effectively displace the coordinated nucleophile. Thus no significant solvent or reverse reaction path was observed in the present systems, such that direct nucleophilic substitution is the major observed reaction pathway under the selected conditions.

The following rate law can be formulated:

$$k_{obsd} = k_2[\text{nucleophile}] \quad (9)$$

where k_2 is a second order rate constant for the forward reaction. The rate law indicates that the reactions proceed *via* a direct nucleophilic substitution pathway. The second order rate constants, obtained from linear least-squares analysis of the kinetic data, Table 2, clearly point to a kinetic preference of $[PtCl(terpy)]^+$ toward the GSH at pH *ca.* 6. 5′-GMP is also a very good nucleophile for Pt(II) complexes, but at neutral pH cannot compete with GSH. The second-order rate constant for GSH is 10^2 times higher for GSH than for 5′-GMP. This is also reflected in the competition reactions utilizing mixtures of GSH and GMP. Also, proton and Pt-195 NMR data did not show any N7 coordination of GMP, in spite of its excess, in the presence of thiols.[12]

However, at or near neutral pH, although less than 10% of thiols are deprotonated, the N-bonding bases cannot compete with the thiol containing amino acids and peptides.[30,12] Therefore, binding primarily takes place through the sulfur donor sites. However, for the GSMe system, rapid coordination to the sulfur atom followed by migration to the N7 site of the purine was observed.[14,18] Similar competition experiments of the bifunctional platinum complex, *cis*-dichloro(ethylendiamine)–platinum(II) and its hydrolyzed forms with a mixture of 5′-GMP or dGpG and thioether containing di- and tri-peptides, also afforded sulfur bound intermediates, followed by the formation of N7 coordinated guanine products.[46,47]

Table 2 Second-order rate constants and activation parameters for the reaction of Pt(II) complexes with nucleophiles.

$[Pt(SMC)(H_2O)_2]^+$				
First reaction				
L	$k_1^{298}/M^{-1}\ s^{-1}$	k_{-1}^{298}/s^{-1}	$\Delta H_1^{\ddagger}$/ kJmol^{-1}	$\Delta S_1^{\ddagger}$/J K^{-1}mol^{-1}
5′-GMP	(22.44 ± 0.82)	0.021	43 ± 2	−76 ± 6
INO	(15.92 ± 0.27)	0.018	—	—
5′-IMP	(10.51 ± 0.24)	0.012	—	—
Second reaction				
L	$k_2^{298}/M^{-1}\ s^{-1}$	k_{-2}^{298}/s^{-1}	$\Delta H_2^{\ddagger}$/ kJmol^{-1}	$\Delta S_2^{\ddagger}$/J K^{-1}mol^{-1}
5′-GMP	(0.24 ± 0.02)	0.0016	59 ± 2	−61 ± 5
INO	(0.17 ± 0.01)	0.0016	—	—
5′-IMP	(0.10 ± 0.01)	0.0012	—	—
$[Pt(terpy)(H_2O)]^{2+}$				
L	$k_1^{298}/M^{-1}\ s^{-1}$	$\Delta H_1^{\ddagger}$/kJ mol^{-1}	$\Delta S_1^{\ddagger}$/J K^{-1} mol^{-1}	
5′-GMP[a]	(6.18 ± 0.09) × 10^2	38 ± 1	−67 ± 2	
5′-IMP[a]	(5.64 ± 0.08) × 10^2	42 ± 1	−54 ± 3	
INO[a]	(4.02 ± 0.07) × 10^2	33 ± 1	−87 ± 3	
GSH[b]	(5.8 ± 0.1) × 10^2	23 ± 1	−116 ± 3	
$[PtCl(terpy)]^+$				
L	$k_2^{298}/M^{-1}\ s^{-1}$	$\Delta H_2^{\ddagger}$/kJ mol^{-1}	$\Delta S_2^{\ddagger}$/J K^{-1} mol^{-1}	
5′-GMP	(9.67 ± 0.46) × 10	43 ± 1	−64 ± 3	
5′-IMP	(7.84 ± 0.17) × 10	—	—	
INO	(9.23 ± 0.22) × 10	—	—	
GSH	(2.18 ± 0.04) × 10^3	36 ± 2	−60 ± 6	
GSH[c]	(4.01 ± 0.17) × 10^3	—	—	

[a] Ref. 30. [b] Ref. 28. [c] Rate constants at 37 °C in the presence of excess of 5′-GMP.

It is important to note that glutathione has been used as a protecting agent and is administered before or after cisplatin.[1,3] Cisplatin readily reacts with glutathione and as much as 67% of the administered platinum has been found to coordinate to glutathione. However, the role of glutathione appears to be dual: glutathione both deactivates and activates cisplatin.[48] The higher effectiveness of cisplatin has also been demonstrated by co-administering cisplatin and glutathione in patients. However, it is not clear whether this increase in effectiveness is due to the reduced toxicity or due to the modification of the platinum drug by binding to the metal. Currently there is much interest in the mechanisms responsible for the development of resistance.

HPLC studies

The progress of the reaction of $[PtCl(terpy)]^+$ with other compounds over extended periods of time can be monitored with techniques such as HPLC, which allows aliquots separated from the reaction mixture at programmed times to be analyzed. The studied reactions were carried out in water, without any buffer, since buffer ions (*e.g.* phosphate) are potential ligands for Pt(II). The pH of each solution was regularly checked over the reaction time, and was shown to be kept between 4.5 and 5.5.

Prior to the study of the reaction between $[PtCl(terpy)]^+$ and glutathione and 5′-GMP, we first reacted the platinum(II) complex with each of the nucleophiles. The products formed were isolated by reversed-phase HPLC and characterized by MALDI-TOF mass spectrometry. As expected, the products obtained corresponded to the adducts $[Pt(terpy)(GS)]^+$ and $[Pt(terpy)(5'\text{-GMP})]^+$ (*m*/*z* 734,2 and 789,8, respectively).

The reaction between $[PtCl(terpy)]^+$, glutathione and 5′-GMP was then followed by HPLC (Fig. 10). The ratio of the three compounds in the repeated assays was 1:1:12, respectively. It was observed that $[PtCl(terpy)]^+$ reacted much faster with glutathione than with 5′-GMP, but this did not prevent a small amount (< 16%) of $[Pt(terpy)(5'\text{-GMP})]^+$ from being formed at the very beginning of the process by reaction of $[PtCl(terpy)]^+$ with some of the large excess of 5′-GMP present in the reaction medium. The relative proportion of this adduct remained virtually constant throughout the reaction process, which indicates that once formed it remains unaltered. The possibility that $[Pt(terpy)(GS)]^+$ reacted with the excess of 5′-GMP present in the reaction mixture to give $[Pt(terpy)(5'\text{-GMP})]^+$ can be ruled out, unless glutathione can replace 5′-GMP from $[Pt(terpy)(5'\text{-GMP})]^+$ at the same reaction rate. The identity of the formed adducts was confirmed by mass spectrometric analysis of the products isolated from the reaction mixture by HPLC (Fig. 11).

Conclusions

In conclusion, this investigation demonstrated that N-bonding ligands such as INO, 5′-IMP and 5′-GMP have a high affinity for $[Pt(SMC)(H_2O)_2]^+$ and $[PtCl(terpy)]^+$, which may have important biological implications, since the interactions of Pt(II) with DNA is thought to be responsible for the antitumour activity of platinum drugs. 5′-GMP is more reactive toward Pt(II) complexes than either INO or 5′-IMP. Also 5′-GMP forms the most stable complexes with Pt(II) compared to INO or 5′-IMP.

However, the preference of Pt(II) to coordinate to GSH was demonstrated. The reactions of the Pt(II) complexes with a mixture of GSH and 5′-GMP yielded a product of Pt–GSH. 5′-GMP cannot effectively compete with the thiol to bind platinum (the second order constants are listed in Table 2). In fact, only small amounts of coordinated 5′-GMP were detected in the HPLC trace. These data clearly support the HPLC results that platinum does not significantly bind to 5′-GMP in the presence of thiol containing small amino acids and peptides.[12,14,48]

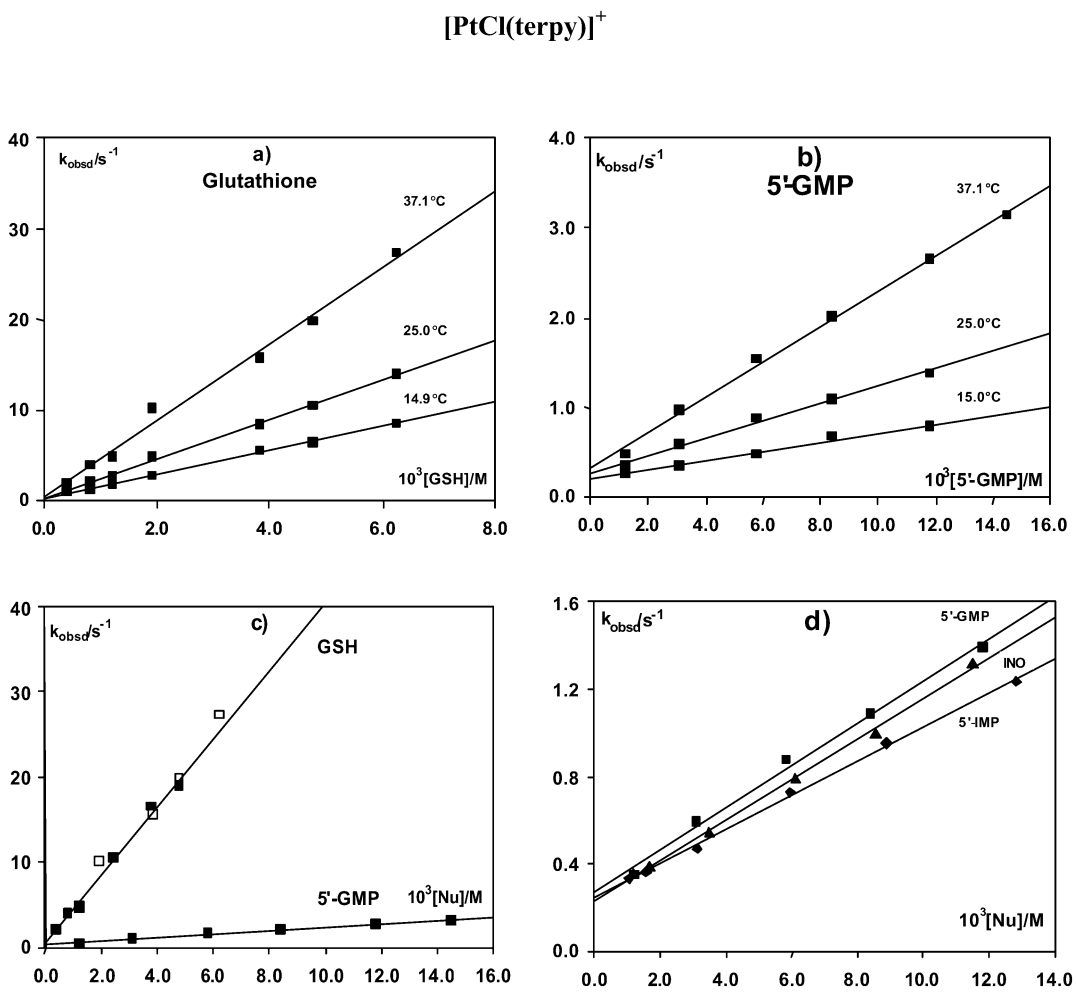

Fig. 9 Observed pseudo-first order rate constants, k_{obsd}, as a function of nucleophile concentration and temperature (a and b); (c) k_{obsd} as a function of nucleophile concentration at 37 °C for 5′-GMP, and GSH without 5′-GMP (□) and in the presence of excess of 5′-GMP (■); (d) k_{obsd} as a function of nucleophile concentration at 25 °C;

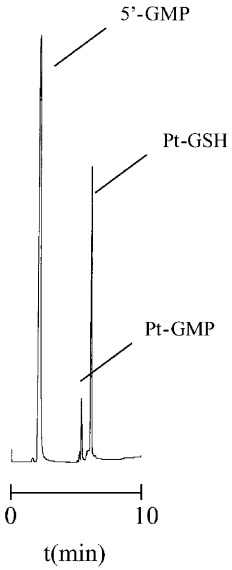

Fig. 10 HPLC profile of an aliquot of the reaction mixture [PtCl(terpy)]$^+$/glutathione/5′-GMP 1:1:12 after 1 week reaction time.

Acknowledgements

The authors gratefully acknowledge financial support from the Ministry of Science, Technologies and Development of the Republic of Serbia, Projects No. 1254, and from the Spanish MEC (grant BQU2001-3693-C02-01) and the Generalitat de Catalunya (2001SGR49, Centre de Referència de Biotecnologia and PIV2001-2). Also, Ž. D. B. thanks the University of Barcelona for a fellowship.

References

1 *Cisplatin, Chemistry and Biochemistry of a Leading Anticancer Drug*, ed. B. Lippert, Wiley-VCH, Zürich, 1999.
2 E. Wong and C. M. Giandomenico, *Chem. Rev.*, 1999, **99**, 2451.
3 J. Reedijk, *Chem. Rev.*, 1999, **99**, 2499.
4 E. R. Jamieson and S. J. Lippard, *Chem. Rev.*, 1999, **99**, 2467.
5 M. A. Fuertes, C. Alonso and J. M. Pérez, *Chem. Rev.*, 2003, **103**, 645.
6 R. T. Door, in *Platinum and Other Metal Coordination Compounds in Cancer Chemotherapy*, ed. H. M. Pinedo and J. H. Schornagel, Plenum, New York, 1996, pp. 131–154.
7 C. J. Ziegler, A. P. Silverman and S. J. Lippard, *J. Biol. Inorg. Chem.*, 2000, **5**, 774.
8 P. M. Takahara, C. A. Frederic and S. J. Lippard, *J. Am. Chem. Soc.*, 1996, **1188**, 12309.
9 P. C. Jocelyn, *Biochemistry of the SH Group*, Academic Press, New York, 1972, p. 94.
10 M. Friedman, *The Chemistry and Biochemistry of the Sulfydryl Group in Amino Acids, Peptides and Proteins*, Pergamon, New York, 1973, pp. 52–87.
11 A. E. Clausen, C. E. Kast and A. Bernkop-Schnürch, *Pharm. Res.*, 2002, **19**, 602.
12 J. M. Teuben, M. R. I. Zubiri and J. Reedijk, *J. Chem. Soc., Dalton Trans.*, 2000, 369.
13 R. N. Bose, S. Moghaddas, E. L. Weaver and E. H. Cox, *Inorg. Chem.*, 1995, **34**, 5878.
14 K. J. Barnham, M. I. Djuran, P. d. S. Murdoch and P. J. Sadler, *J. Chem. Soc., Chem. Commun.*, 1994, 721.
15 K. J. Barnham, M. I. Djuran, P. d. S. Murdoch, J. D. Ranford and P. J. Sadler, *Inorg. Chem.*, 1996, **35**, 1065.

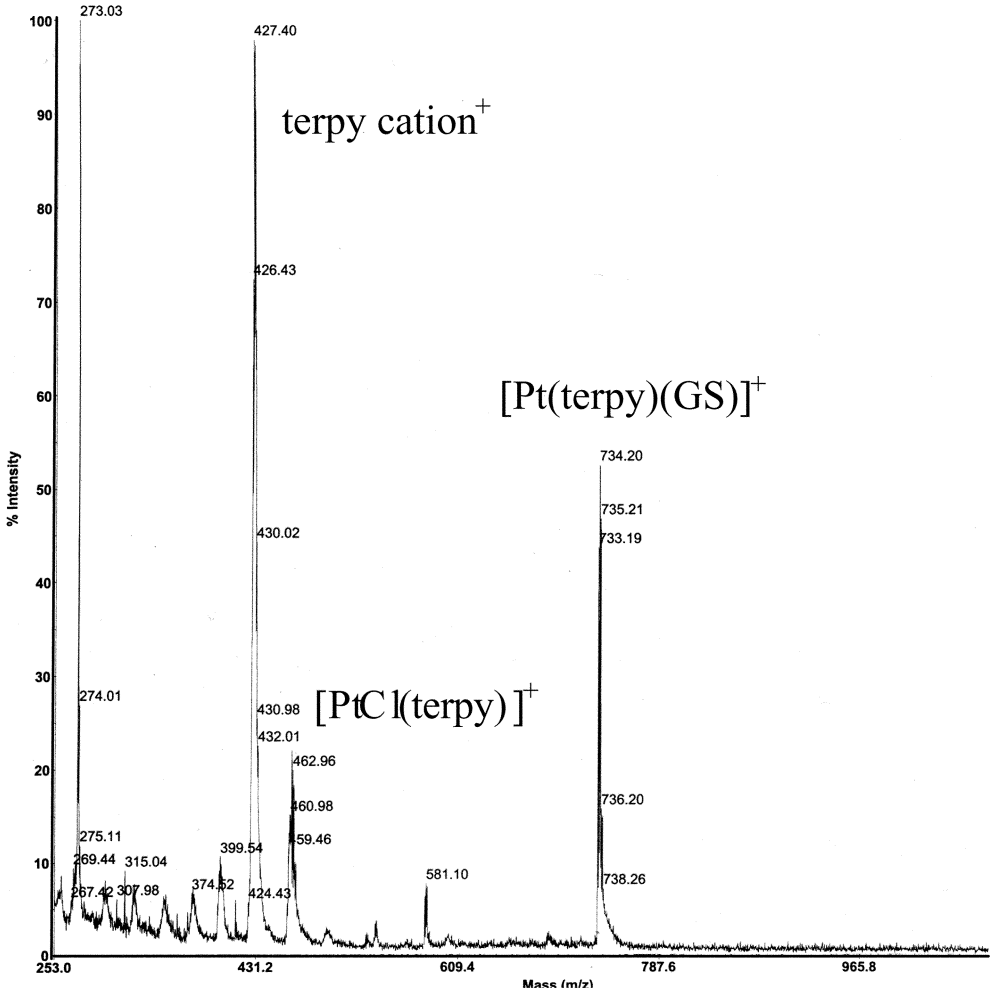

Fig. 11 MALDI-TOF mass spectrum of the adduct $[Pt(terpy)(GS)]^+$ isolated from the reaction mixture $[PtCl(terpy)]^+$/glutathione/5′-GMP 1:1:12.

16 U. Frey, J. D. Ranford and P. J. Sadler, *Inorg. Chem.*, 1993, **32**, 1333.
17 E. L. M. Lempers and J. Reedijk, *Adv. Inorg. Chem.*, 1991, **37**, 175.
18 S. S. G. E. van Boom, B. W. Chen, J. M. Tauben and J. Reedijk, *Inorg. Chem.*, 1999, **38**, 1450.
19 M. Hahn, D. Walters, W. S. Sheldrick, F. B. Hulsbergen and J. Reedijk, *J. Biol. Inorg. Chem.*, 1999, **4**, 412.
20 V. Marchán, V. Moreno, E. Pedroso and A. Grandas, *Chem. Eur. J.*, 2001, **7**, 808.
21 (*a*) D. Jaganyi, A. Hofmann and R. van Eldik, *Angew. Chem., Int. Ed.*, 2001, **40**, 1680; (*b*) A. Hofmann, D. Jaganyi, O. Q. Munro, G. Liehr and R. Van Eldik, *Inorg. Chem.*, 2003, **42**, 1688.
22 B. Pitteri, G. Marangoni, F. V. Viseutim, L. Cattalini and T. Bobo, *Polyhedron*, 1998, **17**, 475.
23 G. Annibale, M. Brandolisio, Ž. Bugarcic and L. Cattalini, *Transition Met. Chem.*, 1998, **23**, 715.
24 B. V. Petrovic, M. I. Djuran and Ž. Bugarcic, *Met.-Based Drugs*, 1999, **6**, 355.
25 K. W. Jennette, S. J. Lippard, G. A. Vassiliades and W. R. Bauer, *Proc. Natl. Acad. Sci. USA*, 1974, **71**, 3839.
26 M. Casummano, M. L. Di Pietro, A. Giannetto and F. Romano, *Inorg. Chem.*, 2000, **39**, 50.
27 G. Annibale, L. Cattalini, A. Cornie, A. Fabretti and F. Guidi, *Inorg. React. Mech.*, 2000, **2**, 185.
28 Ž. D. Bugarcic, G. Liehr and R. van Eldik, *J. Chem. Soc., Dalton Trans.*, 2002, 2825.
29 Ž. D. Bugarcic, G. Liehr and R. van Eldik, *J. Chem. Soc., Dalton Trans.*, 2002, 951.
30 Ž. D. Bugarcic, F. W. Heinemann and R. van Eldik, *Dalton Trans.*, 2004, 279.
31 G. Annibale, M. Brandolisio and B. Pitteri, *Polyhedron*, 1995, **14**, 451.
32 V. Theodrou, I. Photaki, N. Hadjiliadis, R. W. Gellert and R. Bau, *Inorg. Chim. Acta*, 1982, **60**, 1.
33 Ž. D. Bugarcic, M. M. Shoukry and R. van Eldik, *J. Chem. Soc., Dalton Trans.*, 2002, 3945.
34 T. G. Appleton, J. R. Hall, S. F. Ralph and C. S. M. Thompson, *Inorg. Chem.*, 1984, **23**, 3521.
35 R. G. Bates, *Determination of pH-Theory and Practice*, Wiley Interscience, New York, 2nd edn., 1975.
36 J. G. Stark, H. G. Wallace, *Chemistry Data Book*, Murray, London, 1975, p. 75.
37 G. A. Jefersson, *OLIS Kinetic Fitting Program*, OLIS Inc., 1988.
38 P. Gans, A. Sabatini and A. Vacca, *J. Chem. Soc., Dalton Trans.*, 1985, 1195.
39 L. Pettit, University of Leeds, *Personal Communication*.
40 M. Shoukry and R. van Eldik, *J. Chem. Soc., Dalton Trans.*, 1996, 2673.
41 E. M. A. Ratilla, H. M. Brothers and N. M. Kostic, *J. Am. Chem. Soc.*, 1987, **109**, 4592.
42 H. Sigel, S. S. Massoud and N. A. Corfu, *J. Am. Chem. Soc.*, 1994, **116**, 2958.
43 R. B. Martin, *Acc. Chem. Res.*, 1985, **18**, 32.
44 J. Arpalahti and P. Lehikoinen, *Inorg. Chem.*, 1990, **29**, 2564; J. Arpalahti and B. Lippert, *Inorg. Chem.*, 1990, **29**, 104; J. P. Caradonna and S. J. Lippard, *Inorg. Chem.*, 1988, **27**, 1454; R. N. Bose, R. D. Cornelius and R. E. Viola, *J. Am. Chem. Soc.*, 1986, **108**, 4403.
45 M. L. Tobe and J. Burgess, *Inorganic Reaction Mechanisms*, Addison Wesley Longman Inc., Essex, 1999, p. 70.
46 K. J. Barnhham, Z. J. Guo and P. J. Sadler, *J. Chem. Soc., Dalton. Trans.*, 1996, 2867.
47 T. Ishikawa and F. Alli-Osman, *J. Biol. Chem.*, 1993, **268**, 20116.
48 E. Valckova, L. P. Dudones and R. N. Bose, *Pharm. Res.*, 2002, **19**, 124.